

## Integration of remote sensing, airborne geophysics and structural analysis to geological mapping: a case study of the Vieirópolis region, Borborema Province, NE Brazil

*Integração de sensoriamento remoto, aerogeofísica e análise estrutural no mapeamento geológico: estudo de caso da região de Vieirópolis, Província Borborema, Nordeste do Brasil*

José Ferreira de Araújo Neto<sup>1</sup> , Glenda Lira Santos<sup>1</sup> , Igor Manoel Belo de Albuquerque e Souza<sup>1</sup>,  
Sandra de Brito Barreto<sup>2</sup> , Lauro César Montefalco de Lira Santos<sup>2</sup> , João Pedro Santana Bezerra<sup>1</sup>,  
Thais Andressa Carrino<sup>2</sup> 

<sup>1</sup>Programa de Pós-Graduação em Geociências, Universidade Federal de Pernambuco - UFPE, Centro de Tecnologia e Geociências, Avenida da Arquitetura, s/n., CEP 50740-550, Recife, PE, BR (neto.araujo2@hotmail.com; glendaliraa@gmail.com; igor.manoel.belo@gmail.com; jpsbezerra@hotmail.com)

<sup>2</sup>Departamento de Geologia, UFPE, Recife, PE, BR (sandradebritobarreto@gmail.com; lauromontefalco@gmail.com; thais.carrino@gmail.com)

Received on November 21, 2017; accepted on August 05, 2018

### Abstract

This study integrates ASTER GDEM, airborne geophysical data (magnetometry and gamma-ray spectrometry) and field relationships to the geological mapping of units, domains and structures of the Vieirópolis region, State of Paraíba, northeast of Brazil. This area is known for the occurrence of gem-grade and industrial minerals, such as emerald and amazonite. It is inserted in the Rio Grande do Norte Sub-province of the Borborema Province, which is a structurally complex orogenic belt that is in continuity with the Western African mobile belts. The integrated approach revealed that the region is made up of basement rocks intensely deformed by NE-SW transcurrent shear zones. Six main lithological units and three newly mapped shear zones (*i.e.*, Vieirópolis, Lastro and São Pedro) were identified, as well as the expression of the NE-SW-trending Portalegre Shear Zone. The latter controls the occurrence of emerald-bearing phlogopite schists. Magnetic and field data suggest that this major shearing system affects the edge of the Brejo das Freiras Sub-basin as well as syn-kinematic granites. NW-SE, ESE-WNW and E-W lineaments were correlated with late brittle structures that cross-cut the regional foliation and host pegmatite dykes. These results demonstrate the importance of integrating remote sensing, geophysics and field data to constrain the local geology of strongly deformed regions.

**Keywords:** Remote sensing; Gamma-ray spectrometry; Magnetometry; Geological mapping; Borborema Province.

### Resumo

Este estudo integra ASTER GDEM, dados aerogeofísicos (magnetometria e gamaespectrometria) e relações de campo para o mapeamento de unidades, domínios e estruturas geológicas da região de Vieirópolis, Paraíba. Essa área é conhecida pela ocorrência de minerais gemológicos e industriais, tais como esmeralda e amazonita. Está inserida na Subprovíncia Rio Grande do Norte da Província Borborema, a qual é caracterizada como um cinturão orogênico estruturalmente complexo que possui continuidade nas faixas móveis do Oeste Africano. O conjunto de dados integrados revelou que a região é constituída por rochas do embasamento, intensamente deformadas por zonas de cisalhamento transcorrentes NE-SW. Seis unidades litológicas principais e três novas zonas de cisalhamento mapeadas (*i.e.*, Vieirópolis, Lastro e São Pedro) foram identificadas, assim como a expressão da Zona de Cisalhamento Portalegre, de *trend* NE-SW. Essa última controla a ocorrência de flogopita xistos esmeraldíferos. Dados magnéticos e de campo sugerem que esse grande sistema de cisalhamentos afeta a borda da Sub-bacia Brejo das Freiras, bem como granitos sin-cinemáticos. Lineamentos NW-SE, ESSE-WNW e E-W foram correlacionados às estruturas rúpteis menos extensas que cortam a foliação regional e favorecem a acomodação de diques pegmatíticos. Esses resultados demonstram a importância da integração de sensoriamento remoto, geofísica e dados de campo para elucidar a geologia local de regiões fortemente deformadas.

**Palavras-chave:** Sensoriamento remoto; Gamaespectrometria; Magnetometria; Mapeamento geológico; Província Borborema.

## INTRODUCTION

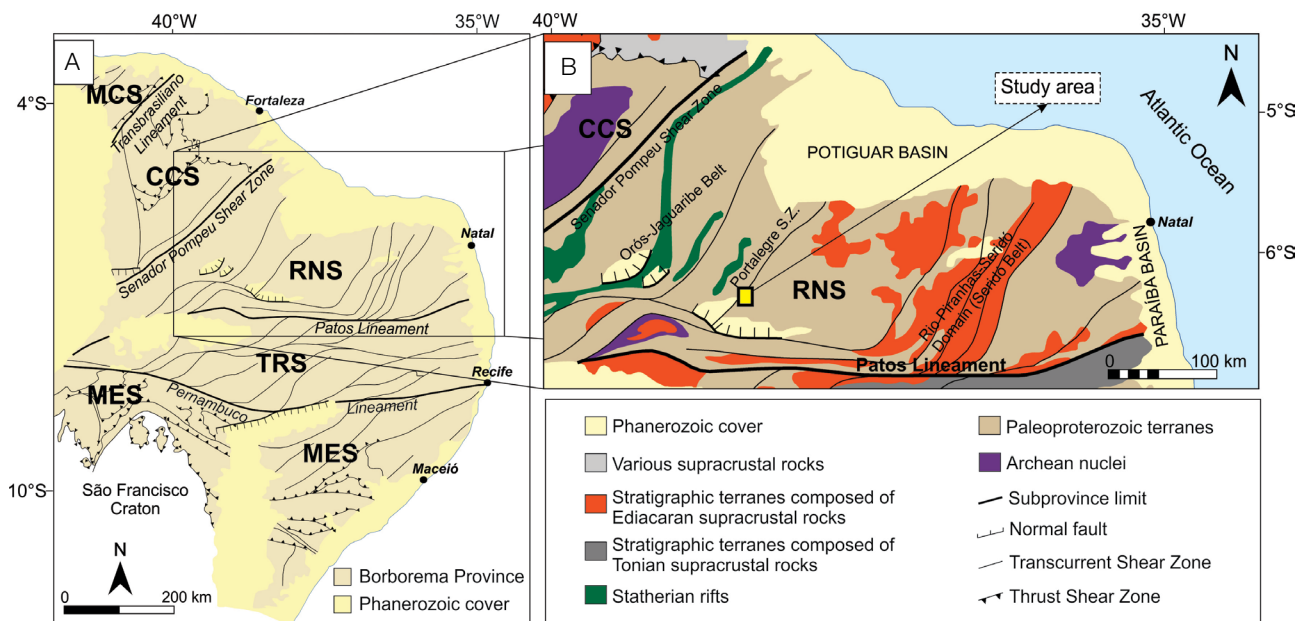
Over the last decades, remote sensing (optical and digital elevation models) and airborne geophysical data have been intensely used to understand the structural evolution of Brazilian provinces (e.g., Dantas et al., 2003; Maas et al., 2003; Madrucci et al., 2003; Carrino et al., 2007; Zacchi et al., 2010). Once they capture data using aerial or orbital sensors, these techniques can rapidly cover a vast area with spatial resolution demanded in mapping on regional or semi-detailed scales.

The integrated interpretation of morphological lineaments derived from digital elevation models, and mesoscopic-scale structural data facilitates the identification and delimitation of important structures, such as shear zones, faults and fractures. Similarly, airborne magnetic and gamma-ray spectrometry images associated with fieldwork data are valuable tools in accurately indicating geological shallow and deep structural markers as well as possible lithological variations (e.g., Dickson and Scott, 1997; Gunn, 1997; Airo, 2013; Ribeiro et al., 2013). Hence, the combination of multiple indirect mapping techniques with fieldwork data has proven to be a valuable tool for the investigation of the crust (e.g., Medeiros et al., 2011; Santos et al., 2017), even in poorly exposed regions (Stewart et al., 2009).

The Borborema Province (BP), in the northeast of Brazil, is characterized by a complex structural array affected by

several deformational, magmatic and metamorphic events spanning almost entirely the Precambrian (Brito Neves et al., 2000). Extensive shear zones and lineaments divide the BP into five sub-provinces (Figure 1A). The Veirópolis region is inserted in the northwest of the State of Paraíba and represents a small area of the Rio Grande do Norte Sub-province (RNS), following the regional trend of the Portalegre Shear Zone (Figure 1B). In this region, geographic conditions, including the semi-arid climate, thin soil cover and mostly dry vegetation, favour the exhibition of large outcrops of crystalline rocks. Previous studies suggest that this area has a promising future in the mining of gem-grade and industrial minerals, including occurrences of emerald-bearing phlogopite schists and amazonite-bearing pegmatites, mostly affected by the Ediacaran Brasileiro deformation (Moraes, 1999; Barreto et al., 2016).

In this paper, we integrate orbital, aerogeophysical and fieldwork data to constrain the tectonic and structural framework of this strongly deformed region as well as delimit its geological units and demonstrate field relationships between major structures and gem mineralization, as shown in other provinces/areas (Paradella et al., 1997; Hoff et al., 2002; Medeiros, 2008; Medeiros et al., 2011). Our final goal is to present a final geological map for the area, based on the integrated analysis of gamma-ray spectrometry, magnetometry and orbital digital elevation model (DEM) data with fieldwork evidence.



MCS: Médio Coreaú Sub-province; CCS: Ceará Central Sub-province; RNS: Rio Grande do Norte Sub-province; TRS: Transversal Sub-province; MES: Meridional Sub-province. Source: modified after Santos et al. (2014).

**Figure 1.** Tectonic division of the Borborema Province (A), highlighting the localization of the study area in the Rio Grande do Norte Sub-province (B).

## GEOLOGICAL SETTING

The BP is located in northeast Brazil and covers an area of approximately 400,000 km<sup>2</sup>, being a wide exposure of Precambrian rocks (Almeida et al., 1981). It is bordered to the south by the São Francisco Craton, to the west by the Parnaíba Basin and to the north and east by coastal basins. It consists of a gneiss-migmatitic basement with ages ranging from the Archean to the Paleoproterozoic, covered and/or interleaved with Meso- to Neoproterozoic domains dominated by supracrustal sequences, which were intensely deformed during the Brasiliano-Pan African Orogeny (800–500 Ma, Brito Neves et al., 2014).

This province is divided into five sub-provinces: Médio Coreau, Ceará Central, Rio Grande do Norte, Transversal and Meridional (Brito Neves et al., 2000; Van Schmus et al., 2008, 2011; Santos et al., 2014). According to these authors, the sub-provinces are limited by lineaments or shear zones, which vary in scale from regional to continental. In the last few decades, two models have been used to explain the consolidation of the province. According to various authors, including Santos (1996), Oliveira (2008), Brito Neves et al. (2000, 2014), Padilha et al. (2016), and Santos et al. (2017), the province represents a complex Neoproterozoic accretionary orogenic system. Alternatively, Neves et al. (2009, 2017) and Neves (2015) propose that the province was consolidated via intracontinental orogenesis and deformation.

The Rio Grande do Norte Sub-province is a Rhyacian to Orosirian crustal block bordered to the south by the Patos Lineament and to the west by the Senador Pompeu Shear Zone (Brito Neves et al., 2000). According to Jardim de Sá (1994) and Medeiros (2008), this sub-province was affected by three main tectonic events. The first ( $D_1$ ) is associated with high-grade orthogneisses, with foliation transposition and development of isoclinal and intrafolial folds. The second event ( $D_2$ ) is related to tangential tectonics coeval with the deposition of the Seridó Group and the intrusion of G2 granitoids of the Poço da Cruz Suite. The  $D_3$  deformation is characterized by the development of extensive Brasiliano transcurrent shear zones.

The main domains that compose the RNS are São José do Campestre, Rio Piranhas-Seridó and Jaguaribeano (Brito Neves et al., 2000; Angelim et al., 2006; Medeiros, 2008). This study area is located in the boundary between the Jaguaribeano (west) and Rio Piranhas-Seridó (east) domains, which are bordered by the Portalegre Shear Zone (PASZ, Brito Neves et al., 2000). This structure represents a crustal discontinuity extending from the Patos Lineament to south, to the Potiguar Basin to the north.

The Jaguaribeano and Rio Piranhas-Seridó domains are mainly represented by Paleoproterozoic basement high-grade metamorphic rocks of the Jaguaretama and Caicó complexes, respectively (Gomes et al., 2000; Ferreira

and Santos, 2000). According to Angelim et al. (2006) and Medeiros (2008), the Jaguaretama Complex is composed of Rhyacian orthogneisses and paragneisses, whereas the Caicó Complex presents two main facies:

1. an older metavolcanosedimentary unit;
2. a younger metaplutonic one.

The whole region was affected by multiple granitic intrusions during the Brasiliano-Pan African Orogeny, which are associated with large-scale transcurrent shear zones.

Lastly, the Brazilian Geological Survey (Medeiros, 2008; Souza et al., 2011) uses the terms Itaporanga and Dona Inês intrusive suites to group and classify the granitoids of the Vieirópolis in regional maps. Nascimento et al. (2015) classify these plutonic rocks as part of the Porphyritic High-K Calc-alkaline Suite and the Equigranular High-K Calc-alkaline Suite, respectively. In this paper, we prefer to define a new nomenclature conforming local toponyms, since no geochemical data is available to fit such rocks in a regional classification.

## MATERIALS AND METHODS

Digital elevation model and airborne geophysical images were used in this study, as well as data collected during fieldwork and geological maps at a scale of 1:250,000 (Sousa Sheet SB.24-Z-A; Medeiros et al., 2005) and 1:100,000 (Pau dos Ferros Sheet SB.24-Z-A-II; Souza et al., 2011), to produce a semi-detailed geological map of the study area. The longitudinal and latitudinal limits expressed in UTM coordinates are, respectively, 575000–590000 m W and 9275000–9295000 m S, 24S zone, in WGS84 horizontal projected *datum*.

The study of topographic lineaments by remote sensing was carried out using the Global Digital Elevation Model (GDEM) of the Advanced Spaceborne Thermal Emission and Reflection Radiometer (ASTER) sensor. The image (ASTGDEM2\_0S07W039) was acquired on October 17<sup>th</sup>, 2011, and was taken from the United States Geological Survey website (<http://earthexplorer.usgs.gov/>), in GeoTiff format of 3,601 x 3,601 pixels and 30-m spatial resolution. High-pass convolution filters (directional edge) from a Kernel 3 x 3 matrix were applied to the GDEM ASTER image to emphasize the structures parallel to the direction of each filter (Drury, 2001). Directional filters were applied for the azimuths 0°, 45°, 90°, 135°, 180°, 225°, 270° and 315° for a comprehensive cover of the area, using the ENVI software. Visual interpretation of lineaments was carried out using ArcMap software at a 1:100,000 scale, tracing ridge crests and linear drainage features. For each vector created, the azimuthal direction and the length were noted in order to produce a rose diagram. To group these features,

the classification used by Batista et al. (2014) was adopted, where the N-S and E-W limits comprise a margin of 10° in clockwise and anti-clockwise directions.

The airborne magnetic and gamma-ray spectrometric data used in this study were taken from the Paraíba–Rio Grande do Norte Airborne Geophysical Project (CPRM, 2009), carried out by the Brazilian Geological Survey in partnership with LASA and PROSPECTORS companies, also responsible for data processing. This survey was carried out between 1/31/2009 and 9/10/2009, with a nominal flight altitude of 100 m. The spacing between N-S flight lines and E-W control lines comprises, respectively, 0.5 and 10 km. The 125-m cell size grids of anomalous magnetic field and radioelements (K, eTh, eU and total count) were obtained by the application of bidirectional techniques and minimum curvature, respectively. They were windowed for the study area of 300 km<sup>2</sup> using the Oasis Montaj software. To observe structures on a regional scale, aeromagnetic grids were windowed for an enlarged SW area reaching 1,125 km<sup>2</sup>. The first vertical derivative (DZ) and 3D analytic signal amplitude (ASA) filters were applied to the anomalous magnetic field map using the Oasis Montaj software. These filters enhance the contrast of magnetic susceptibility associated with different sources observed in the region, facilitating the interpretation of magnetic lineaments. The vertical derivative highlights change in the vertical direction of the potential field, enhancing high frequencies relative to low frequencies, eliminating long-wavelength regional effects (Milligan and Gunn, 1997). The 3D analytic signal amplitude is a filter of high centrality and consists of the square root of the sum of squares of the directional derivatives for the x, y, and z directions of the anomalous magnetic field. This filter allows the centralization of maximum amplitudes over the anomalous sources (Roest et al., 1992), and has low dependence on total magnetization direction and the position of the study area to the magnetic Equator. The visual interpretation of magnetic lineaments in the DZ and ASA images was performed using the Oasis Montaj software at a 1:150,000 scale. The main trends were delineated at the border of magnetic anomalies, which suggests structural or lithological contrasts in the subsurface. Maps for potassium (K), equivalent thorium (eTh) and equivalent uranium (eU) channels of the gamma data, as well as for the total count, were also used. A ternary map of K, eTh and eU in the RGB (Red, Green, Blue) composition was produced and used to interpret lithogeophysical domains.

The local geological mapping was carried out at a scale of 1:50,000 during five field trips in May, August and December 2015, February 2016 and February 2017. Lithological and structural data were obtained from 417 outcrops described. The final geological map was produced by integrating fieldwork, petrographic and structural data, and the interpretation of digital images.

## RESULTS AND DISCUSSION

### Remote sensing

The application of directional filters (0°, 45°, 90°, 135°, 180°, 225°, 270° and 315°) on the ASTER GDEM image generated eight new images (Figure 2), each one enhancing topographic features parallel to the filter direction, which allowed the tracing of multiple topographic lineaments grouped in four different direction classes: N-S, E-W, NE-SW, NW-SE. Lineaments between N10W and N10E (350° to 10° Azimuth) are considered to be N-S, and those between N80E and S80E (80° to 100° Azimuth) are considered to be E-W. The orientations between these intervals were classified as NE-SW (N11E to N79E) or NW-SE (N11W to N79W).

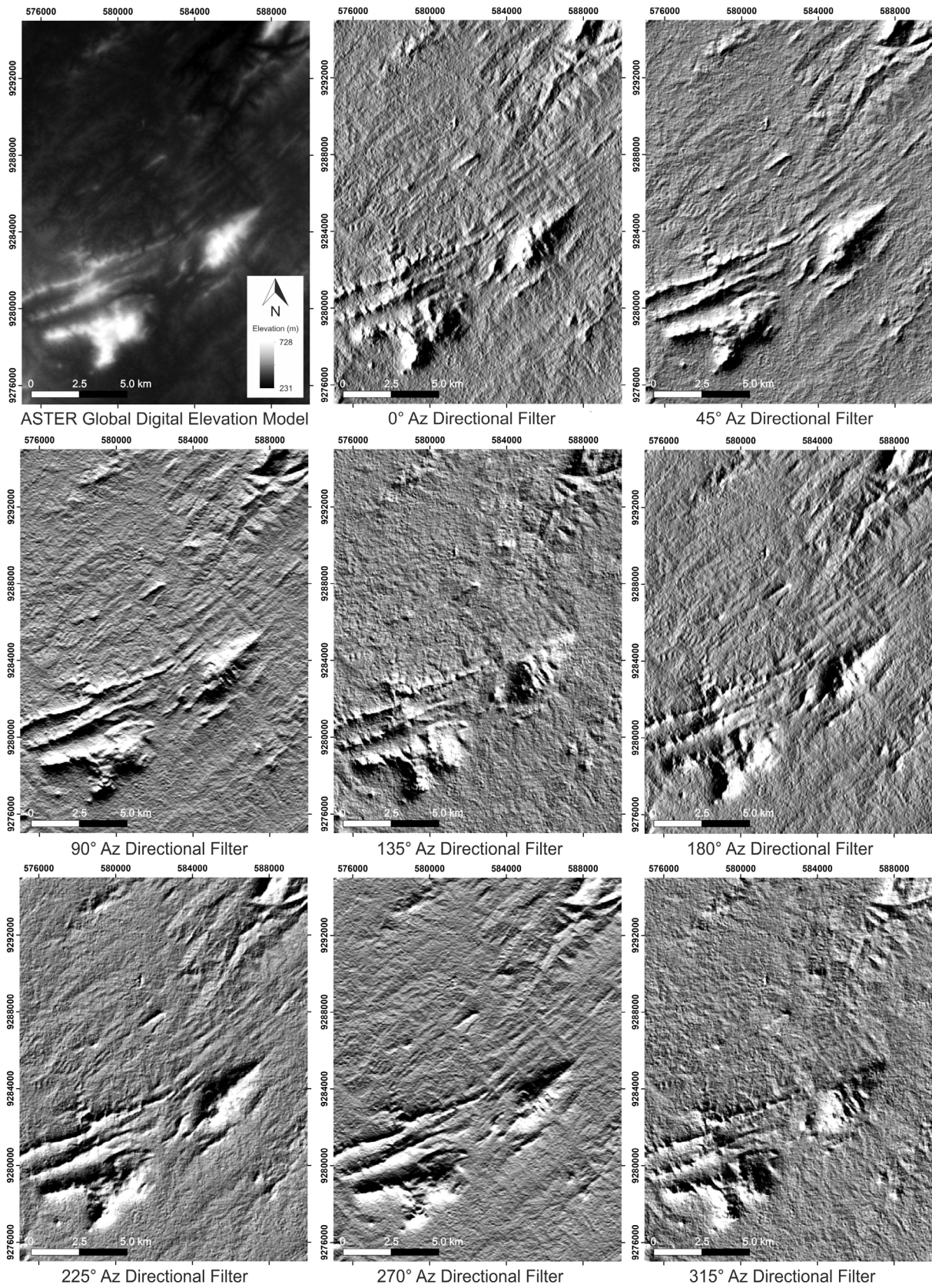
From the 298 interpreted lineaments, 58% follow a NE-SW trend, with an average length of 1,421 m, whilst the NW-SE trend represents about 30% of interpreted lineaments with an average length of 1,548 m (Table 1). The remaining 6% correspond to N-S or E-W lineaments. Figure 3A shows the distribution of the interpreted lineaments superimposed to the results arising from directional filtering in 45 and 135° Az (both images having 50% transparency). The strong NE-SW orientation is marked by dense lineament traces throughout the study area, mostly parallel to high topographical prominences. This main trend is cross-cut and offset by the extensive NW-SE and less frequent E-W lineaments, which occur in topographic valleys. The rose diagram in Figure 3B shows that the main NE-SW trend is essentially oriented in the 40 to 50° Az direction with the secondary NW-SE trend mostly perpendicular (310 a 320° Az) to the NE-SW trend, whilst N-S and E-W directions are less expressive in the study area.

### Magnetometry

The visual interpretation of the main magnetic lineaments was carried on the first vertical derivative of anomalous magnetic field (Figure 4B) and analytic signal amplitude images (Figure 4C). The latter image shows strong magnetic anomalies in the west-central and southwestern areas. In both products, preferred orientation lineaments of NE-SW direction are found widespread along the entire area. These extensive NE-SW lineaments are mostly associated with strong magnetic contrasts, while subtle discordant E-W, WNW-ESE and NW-SE lineaments may cross-cut and truncate the main direction trend.

### Gamma-ray spectrometry

Maps of K (%), eTh (ppm) and eU (ppm), as well as total count channel (μR/h), and the ternary composition RGB of the radioelements are shown in Figure 5. High K contents

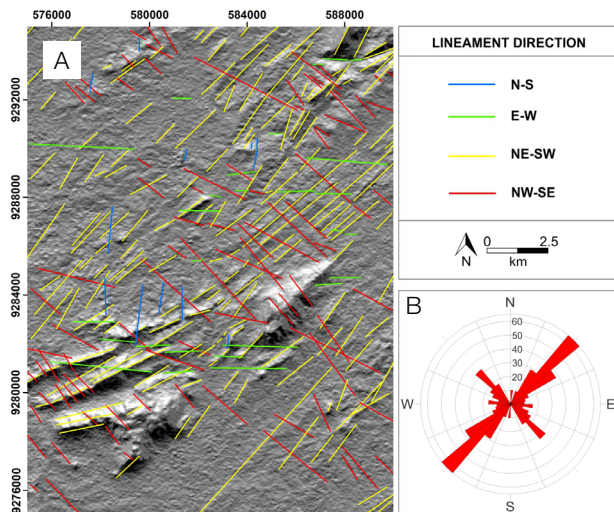


**Figure 2.** Results of the directional filtering technique applied to ASTER GDEM images.

**Table 1.** Classification of lineaments interpreted from filtered ASTER GDEM images.

Lineament direction	N° of lineaments	Range (m)	Average length (m)
NE-SW	170 (57%)	150–8,160	1,421
NW-SE	91 (30%)	310–4,752	1,548
E-W	26 (9%)	382–4,319	1,519
N-S	11 (4%)	219–2,494	1,060

Total of lineaments = 298.

**Figure 3.** Main interpreted lineaments from the filtered ASTER GDEM image (A) and respective rose diagram (B).

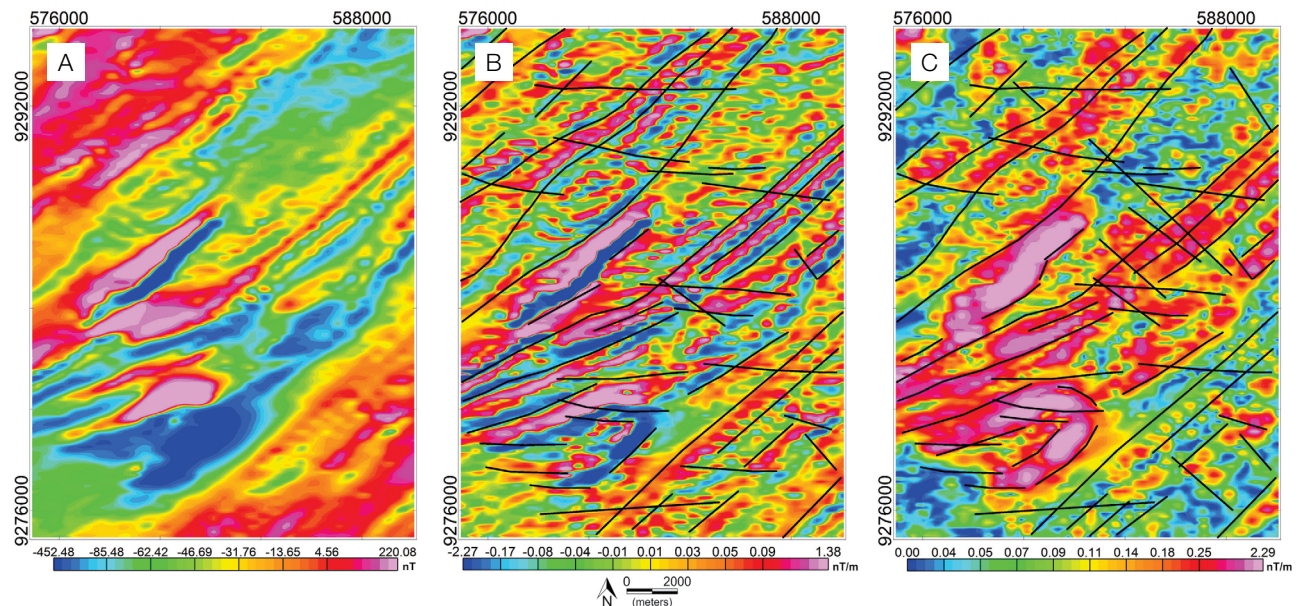
occur in the southwest, central-east and northeast sectors of the study area (Figure 5A). eU and eTh values are similarly distributed, usually being higher in the north sector of the area, and lower in the south (Figures 5B and 5C). Regions with low values for the three radioelements occur as arranged zones in the NE-SW direction, suggesting a strong link with the structures observed in the field. This pattern is also present in the total count map (Figure 5D).

Twelve lithogeophysical domains were determined by visual analysis of relative K, eTh and eU contents using the ternary map shown in Figure 5E. The radioelement contents were interpreted as low (L), medium to low (ML), medium (M), medium to high (MH) and high (H). Domains 1 and 6 show an enrichment of eU in comparison to the other radionuclides. Relatively high values of eTh can be seen in domain 3, whereas the enrichment of K is evident in domain 9. Depleted and enriched areas in the three radioelements are represented, respectively, in domains 5 and 10, whilst intermediate values determine the other domains.

## Geological mapping

### Lithological features

The study area is mainly composed of basement rocks of the Jaguaretama and Caicó Complex, *augen* gneisses of the Poço da Cruz Suite and several intrusive igneous rocks. The Jaguaretama Complex is located to the west of the Portalegre Shear Zone, forming limited outcrops of greyish orthogneisses and meta-granites of monzogranite and

**Figure 4.** Map of (A) anomalous magnetic field and interpretation of magnetic lineaments in the study area from the images of first vertical derivative of anomalous magnetic field (B) and of analytic signal amplitude (C).

granodiorite composition (Figure 6A). Such rocks are made up of plagioclase, quartz, K-feldspar and biotite, whereas epidote, allanite, titanite and apatite are accessory minerals. Protomylonites occur near the Portalegre Shear Zone.

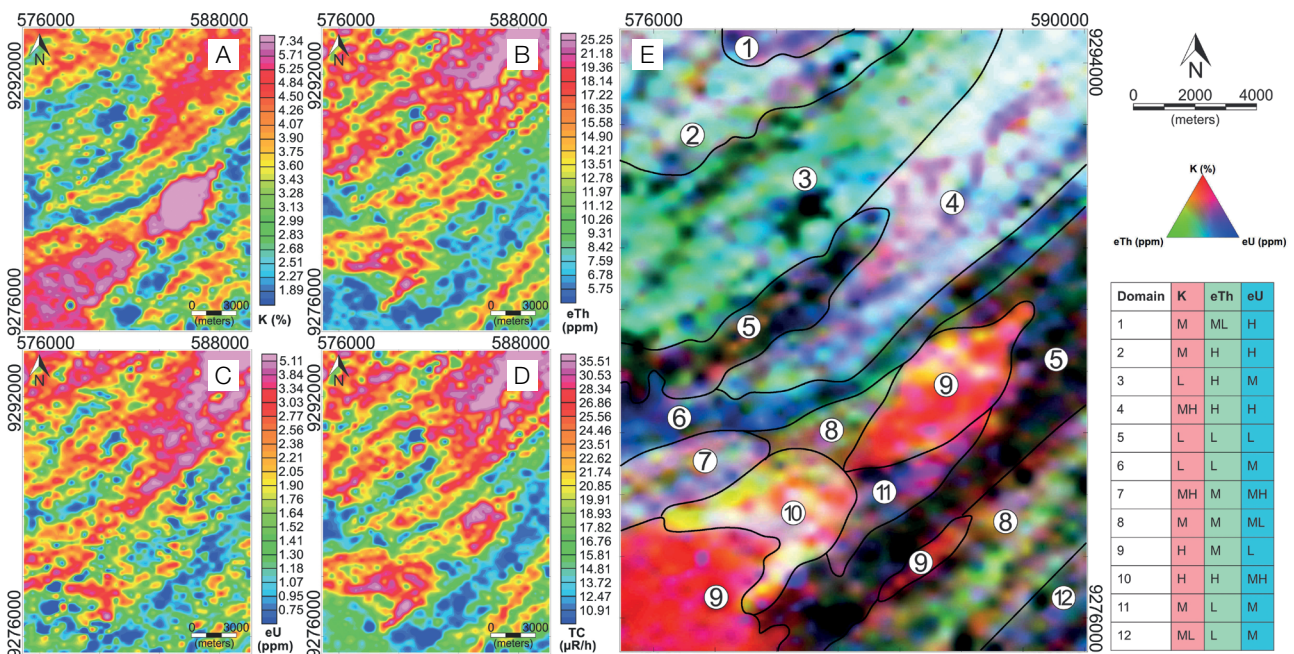
The Caicó Complex is composed of metavolcano-sedimentary and metaplutonic units. The former is made up of amphibolites (Figure 6B), mylonitized quartzites, orthomylonites, biotite/phlogopite schists and paragneisses, whereas the latter is composed of fine-grained orthogneisses of dioritic composition. Further, the metaplutonic unit presents large textural variation, ranging from metagranites, banded orthogneisses (Figure 6C), migmatites, migmatized orthogneisses and proto- to ultramylonites. Fine-grained orthogneisses are greyish and can contain K-feldspar forming *augens*. The migmatites are mainly metatexites showing dilation, *schollen*, stromatic structures and flebitic folds. The protomylonites to ultramylonites occur mainly in the Veirópolis and Lastro shear zones. The composition of orthogneisses and mylonitized rocks vary from syenogranite to tonalite, containing mainly K-feldspar, quartz, plagioclase, hornblende and/or biotite. The associated accessory minerals are allanite, epidote, apatite and less commonly, magnetite.

Inserted in the Caicó Complex, the *augen* gneisses of the Poço da Cruz Suite occur as elongated lenses containing rose K-feldspar porphyroblasts, quartz, microcline, plagioclase and biotite. Epidote and chlorite are the main accessory minerals. Less deformed rocks correspond to the Serra Negra, Serra Branca and Panati granites, which intrude

orthogneisses of the Caicó Complex. The Serra Negra Granite is characterized by syenogranite to monzogranite compositions and is hosted by the Caicó Complex. The rocks are leucocratic and porphyritic, exhibiting whitish and zoned K-feldspar phenocrysts of up to 2 centimetres in length (Figure 6D). The matrix is inequigranular, medium- to coarse-grained and composed of microcline, plagioclase, quartz, hornblende, biotite and titanite. Epidote and carbonates occur as alteration minerals resulting from saussuritization. Centimetre-sized diorite enclaves are present.

The Serra Branca Granite is characterized by monzogranite to quartz monzonite compositions, with light pink or whitish color and fine- to medium-grained inequigranular texture (Figure 6E). The mineralogy comprises quartz, K-feldspar and plagioclase, as well as aegerine-augite, biotite, epidote and titanite as accessory minerals. The Panati Granite occurs in the northeastern sector of the study area in Serra do Panati. This unit crops out as bodies of fine-grained bulging rocks composed of pink to grey syenogranites and granodiorites. Its mineral content is made up of K-feldspar, plagioclase and quartz, having biotite, allanite and muscovite as accessory minerals.

Various pegmatite dykes and veins were identified along the NE-SW shear zones, as well as NW-SE extensional filled sites. Generally, NE-SW pegmatites occur as tabular or irregular bodies parallel and subparallel to the regional foliation, commonly intruding basement rocks. These pegmatites often present a simple composition made up of



L: low; ML: medium to low; M: medium; MH: medium to high; H: high.

**Figure 5.** Maps of K (A), eTh (B), eU (C), total count (TC) (D), and ternary map in RGB composition (K, eTh, eU), classified in lithogeophysical domains (E).

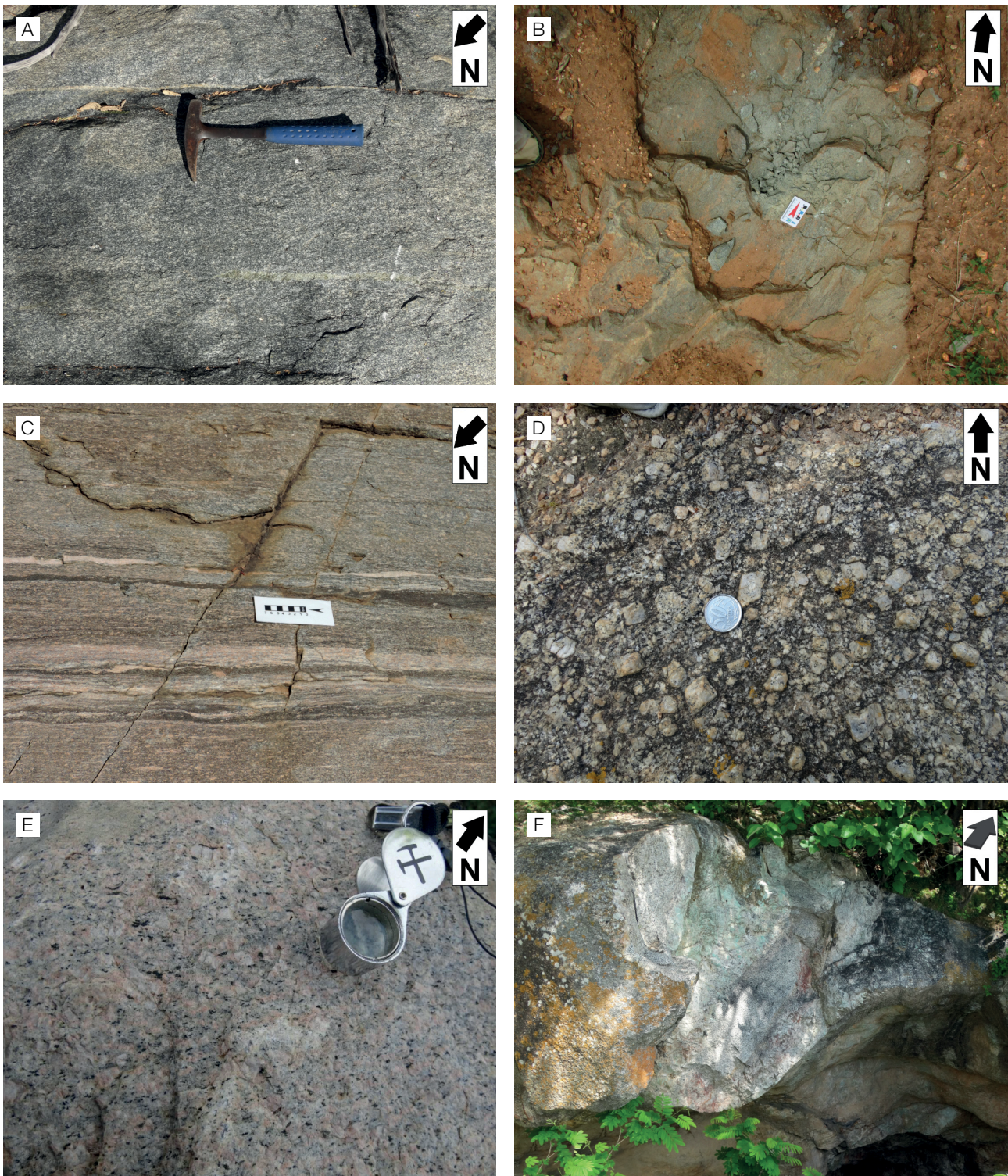


**Figure 6.** (A) Metagranodiorite from the Jaguaretama Complex; (B) incipiently altered amphibolite lens from the Caicó Complex; (C) centimetre-scale gneissic banding from the Caicó Complex, with a mesocratic band of monzogranite composition and a leucocratic band of syenogranite composition; (D) up to 2 cm-sized K-feldspar megacrysts, characterizing the porphyritic texture of the Serra Negra Granite; (E) pink leucogranite from the Serra Branca Granite, marked by euhedral and subhedral K-feldspar crystals and an inequigranular porphyritic texture; (F) amazonite pegmatite lens hosted in the Serra Branca Granite.

quartz, K-feldspar and plagioclase, with or without garnet and/or muscovite. Major NW-SE pegmatites are found cross-cutting the Serra Branca Granite forming lenses or tabular bodies composed of amazonite, plagioclase and quartz, and can contain pink feldspar, biotite, black tourmaline, and beryl (Figure 6F).

### Structural geology

Several NE-SW-trending shear zones were mapped. They are, from northwest to southeast, Portalegre, Vieirópolis, Lastro and São Pedro. The Portalegre Shear Zone is characterized by a dextral transcurrent kinematics, vertical and subvertical foliation planes materialized by mylonitic and protomylonitic foliations, asymmetric lenticular *boudins* and S-C structures (Figure 7A). This shear zone controls the occurrence of several pegmatites and emerald-bearing phlogopite schist lenses, which occur parallel or subparallel to the mylonitic foliation (Figure 7B). The Vieirópolis Shear Zone refers to the most expressive deformation marker of the region and is characterized by mylonites and ultramylonites following the NE-SW direction. Vertical and subvertical foliations and horizontal aligned stretching mineral lineation are observed, as well as various dextral asymmetric *boudins* (Figure 7C). This shear zone strongly affected the migmatites and banded gneisses of the Caicó Complex, creating outcrop-scale isoclinal folds. Additionally, this shear zone is closely related to the Serra Negra Granite, interpreted as syn-kinematic. The Lastro and São Pedro shear zones are less expressive. The Lastro Shear Zone controlled the emplacement of granite bodies and occurs along N50E-trending mylonite zones, with vertical foliation and horizontal mineral lineation (Figure 7D). On the other hand, the São Pedro Shear Zone is also distinguished by a vertical mylonitic foliation, but occurs in the extreme southeast, close to the limits of the study area.

Various stages of late brittle deformation were identified (Figure 7E). They are characterized by fractures filled by K-feldspar and quartz veins that cross-cut the regional foliation, generally in NNW-SSE directions, or parallel to the NE-SW foliation. Later unfilled E-W-, WNW-ESE- and NW-SE-trending fractures and faults also occur, with occasional associated conjugate joints. These extensional sites possibly favoured the rise of pegmatite fluids, resulting, for example, on the formation of amazonite pegmatites in the NE sector of Serra Branca Granite (Figure 7F).

### Data integration

The integrated study allowed us to map six main lithological units and major structures, *i.e.*, the Portalegre Shear Zone in addition to three new shear zones, Vieirópolis, Lastro and São Pedro. The detailed geological map derived from this integrated approach is shown in Figure 8.

The main lineaments interpreted using remote sensing and geophysical maps show a major NE-SW trend associated with the transcurrent Brasiliano shear zones, including the Portalegre structure. The ASTER GDEM image (Figure 3) allowed us to define a NE-SW concordant corridor composed of gneisses and mylonites associated with the Caicó Complex, along the Vieirópolis Shear Zone, marked by syn-kinematic granites. The first derivative and analytical signal amplitude magnetic maps show a strong correlation between these mylonitic rocks with highly positive magnetic anomalies. In a similar way, topographic and magnetic lineaments following the NE-SW direction in the NW sector of the area give support to the field relationships, being associated with the mylonites and the emplacement of pegmatite bodies along the Portalegre Shear Zone, a structure that is directly related to the occurrence of emerald-bearing phlogopite schist lenses. The close relationship between sheared pegmatites veins and phlogopite schist along this shear zone suggests that this structure probably played an important role in channelling hydrothermal fluids containing Be from the pegmatites and Cr from the mafic/ultramafic rocks (metamorphosed into amphibolites), that ultimately produced emerald crystals. The continuity of the Portalegre Shear Zone is well marked, especially on the first vertical derivative map (Figure 4A).

A secondary NW-SE trend and a minor E-W trend represent a late brittle deformation stage evidenced by dense fracturing (Figure 7E), small strike-slip faults and quartz filled fractures. These features are present in the magnetic maps but mostly enhanced in filtered ASTER GDEM images (Figure 2). Hence, the structural pattern of the study area, dominated by NE-SW and NW-SE fabric, controls the drainage system, generating trellis and rectangular patterns in mylonitic units (Caicó Complex) along the Vieirópolis and Lastro shear zones (Figure 9).

The ternary map of radioelements integrated with the filtered digital elevation model (Figure 9) contributes to the delimitation and individualization of lithotypes, which show contrasting K (%), eTh (ppm) and eU (ppm) contents. Despite the 500 m flight line spacing, the airborne gamma-ray spectrometric images allow the individualization of the Serra Branca and Serra Negra granites. The former shows high contents of the three radioelements (Domain 10), whereas the latter is characterized by high concentrations of K (Domain 9). These granites are also discriminated based on their magnetic signature, with the Serra Branca Granite responsible for extremely positive magnetic anomalies in the southwestern sector of the study area.

The Caicó and Jaguaretama complexes also present different radiometric responses, such as low K contents related to the rocks of the Jaguaretama Complex, which occur to the west of the Portalegre Shear Zone, representing the Jaguaribeano Domain basement. Regions with low K, Th and U concentrations (Domain 5) are related to the drainage

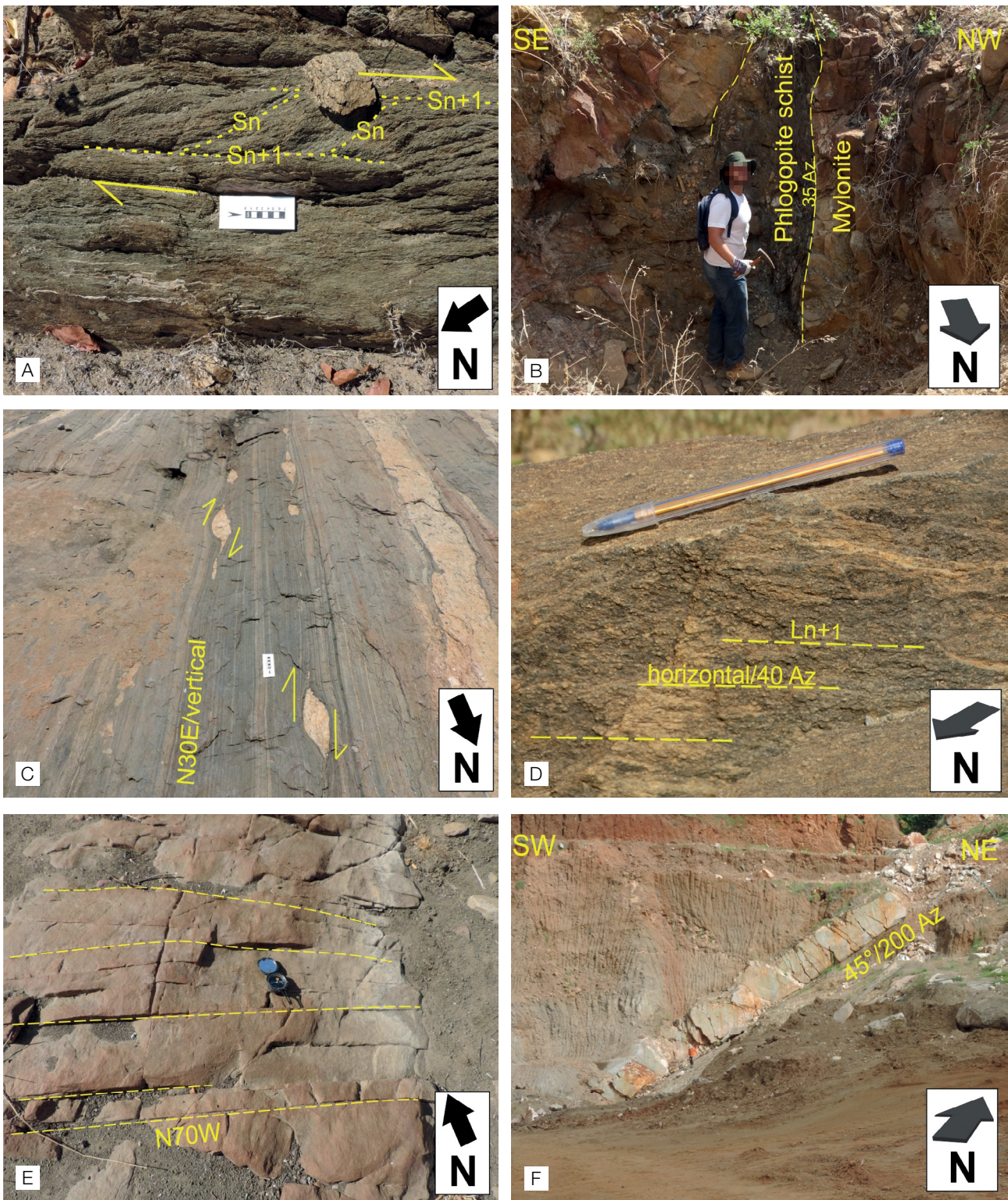


**Figure 7.** (A) S-C structure showing dextral kinematic in biotite-chlorite schist along the Portalegre Shear Zone; (B) emerald-bearing phlogopite schist lens concordant with mylonite along the Portalegre Shear Zone; (C) dextral asymmetrical *boudins* in mylonite along the Vieirópolis Shear Zone; (D) vertical mylonitic foliation and horizontal mineral lineation close to the Lastro Shear Zone; (E) NW-SE late-formed fractures, cutting ultramylonites of the Caicó Complex; (F) mining front of the amazonite pegmatite hosted in Serra Branca Granite, associated with late extensional sites.

system, to mylonitic facies of the Caicó Complex and to the amphibolite lenses which occur generally associated with a thick soil cover. The orthogneisses of the Caicó Complex show a range of radioelement contents that can be related to compositional banding at a regional scale and to different migmatization stages, besides presenting varying K contents due to the quantity of quartz-feldspathic pegmatite intrusions.

Domain 6 is characterized by medium eU and low K and eTh contents (Figure 5). This domain is located along the Vieirópolis Shear Zone (Figure 9), which suggests the possibility that mylonites to ultramylonites of the Caicó Complex have become enriched in uranium due to the loss of volume generated by the loss of elements, such as

silicon and sodium with increasing strain, as suggested by Gundersen (1991) for mylonites along the Brookneal Shear Zone (Virginia, EUA). High eU concentrations in mylonites were also observed by Acharyulu et al. (2004), when studying the behaviour of radioelements in various rock types of the Sambalpur District, India.

Due to the intense deformation along the Vieirópolis Shear Zone and the response of this structure in the remote sensing and airborne geophysical images, regional aeromagnetic maps were analysed to enable the observation of its limits in relation to the Portalegre Shear Zone (Figure 10). The visual interpretation of magnetic lineaments on the first vertical derivative of anomalous magnetic field (Figure 10A), and

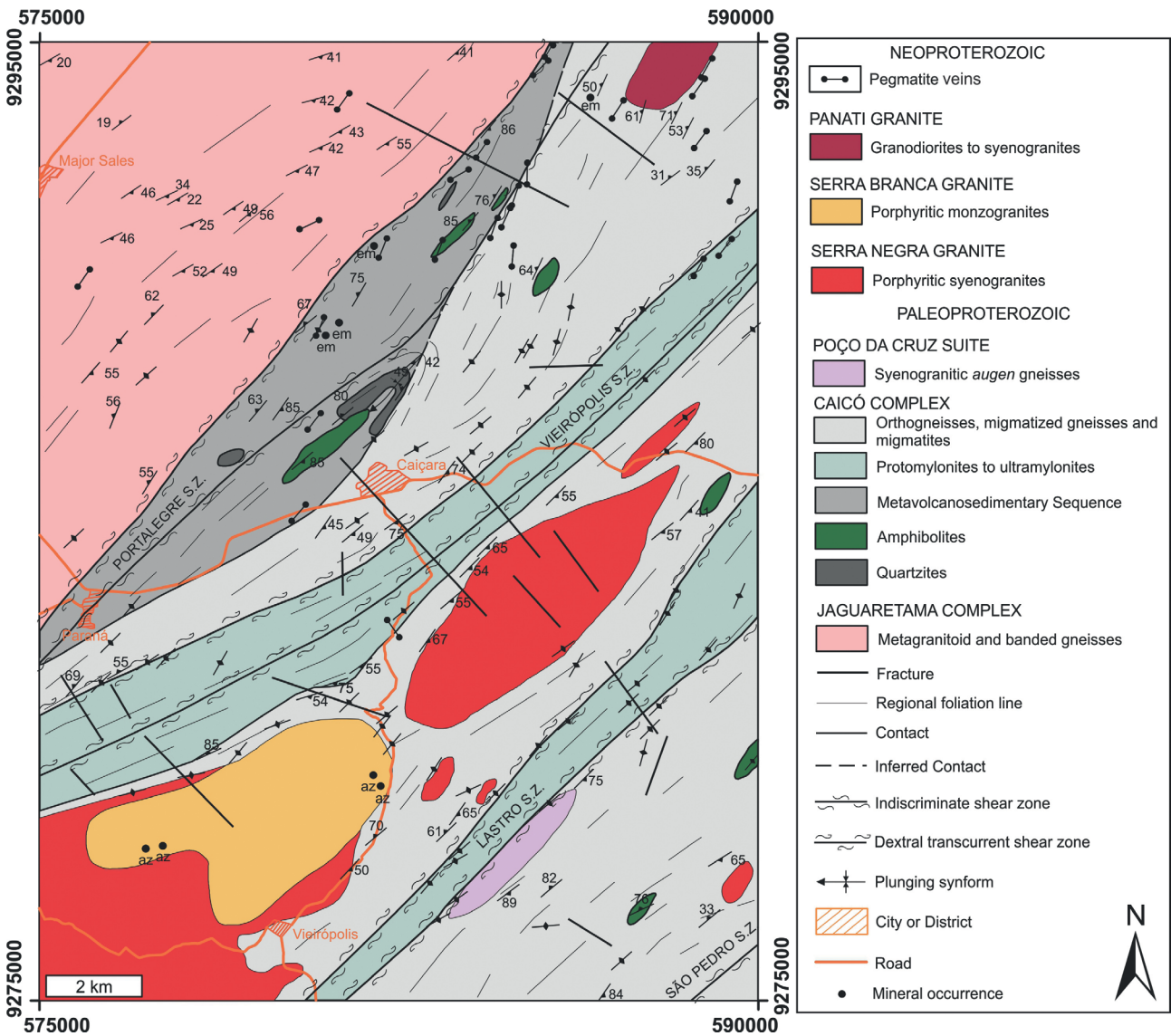


**Figure 8.** Simplified geological map of the Vieirópolis region and surrounding area, produced by the integration of remote sensing and airborne geophysics with field work data.

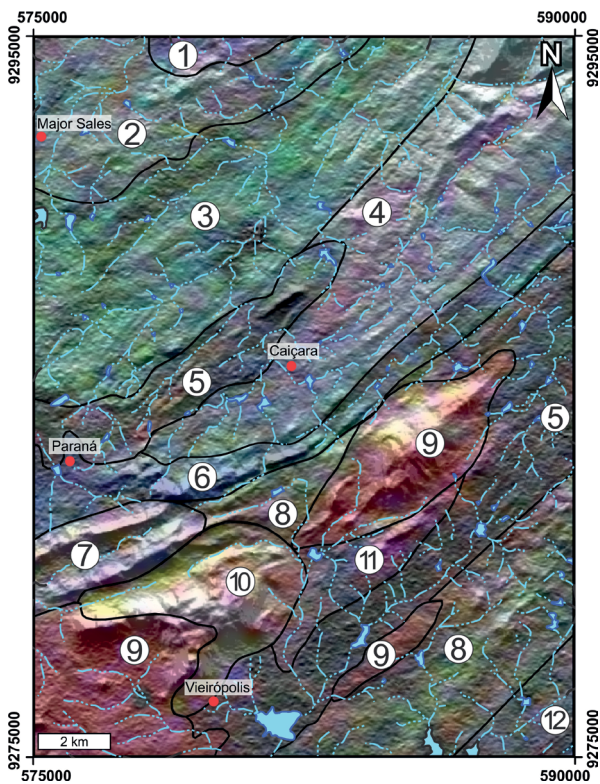


**Figure 9.** Ternary map of K, eTh, eU (RGB), overlaid on the filtered ASTER GDEM image (45 and 135 Az), including interpreted lithogeophysical domains and drainage pattern (light blue). Lithogeophysical domains legend in Figure 5E.

analytic signal amplitude (Figure 10B) indicates that the Vieirópolis Shear Zone is probably a secondary lineament of the Portalegre Shear Zone, originating in the extreme northeast of the edge of the Brejo das Freiras Sub-basin (Rio do Peixe Basin), extending approximately 30 km in a NE-SW direction. Similar structures were mapped by Nóbrega (2004) in the north of the studied area, in Caraúbas region (RN), making up the Portalegre Shear Zone System.

## CONCLUSIONS

The Vieirópolis region is inserted in a highly deformed portion of the Rio Grande do Norte Sub-province, strongly affected by the NE-SW-trending Portalegre Shear Zone. The integrated use of interpreted lineaments from the ASTER GDEM, airborne magnetic and gamma-ray spectrometric images with field work data permitted the tracing and identification of the Portalegre shearing system, besides the pioneering mapping of three new transcurrent shear zones: São Pedro, Lastro and Vieirópolis. These ductile structures control the emplacement of multiple igneous intrusions and the regional foliation trend, generating mylonitic foliations in

the basement rocks of the Jaguaretama and Caicó complexes. In this case study, the integration of direct and indirect data has been shown to be effective to the local geological cartography, in special to delimitate extensive shear zones, foliation traces and late structural features, such as regional fracture systems.

The use of edge detection filters in GDEM image processing allowed the interpretation of 298 lineaments. Most lineaments exhibit NE-SW trend, which reflects the regional framework imposed by the ductile tectonic generated by the transcurrent shear zones of the Brasiliano Orogeny. These structures have a main direction between 40 and 50° Az and deformed packages of Paleoproterozoic rocks, as well as controlled the emplacement of the Serra Branca, Serra Negra and Panati granites and several pegmatite dykes and veins. Continuous lineaments, interpreted on the first vertical derivative and analytic signal amplitude maps, corroborate the existence of these shear zones, which occur associated with subvertical and vertical protomylonitic and ultramylonitic foliations.

The Vieirópolis Shear Zone stands out, compared to the others, because of the intense topographic and magnetic signatures, being associated with mylonites and ultramylonites along a NE-SW trend, which are characterized in the gamma-ray spectrometry by low K and eTh contents and relatively high eU contents, a common pattern in highly deformed rocks. Besides, this shear zone is marked by high positive magnetic anomalies, which extends for, at least, 30 meters and originates on the edge of the Brejo das Freiras Sub-basin, suggesting a structural connection with the Portalegre Shear Zone.

The brittle regime, characterized by fractures and/or faults predominantly in a NW-SE and E-W direction, is subordinated, cross-cutting the main structures. Close to the shear zones, this fracturing pattern is transversal to the mylonitic foliation and controls the local drainage pattern, besides the emplacement of quartz-feldspar veins and tabular pegmatite dykes.

The gamma-ray spectrometry method was used as a complementary data, in order to delimit the main mapped lithologies. This geophysical method enabled to distinguish the Serra Branca from the Serra Negra granite, which can be sometimes difficult in the field. Additionally, various lithogeophysical domains boundaries reflect the strong structural control of the area, which demonstrates that 0.5-km flight-line-spaced geophysical surveys could be a powerful tool even at local scale mapping.

Lastly, regional scale geophysical data and digital elevation models do not allow identification or individualization of small (metre-sized) mineralized bodies, such as emerald-bearing phlogopite schists and amazonite pegmatites. Instead, one can delimitate regional structures responsible for the mineralization control, which is the first step to understand local mineralization.

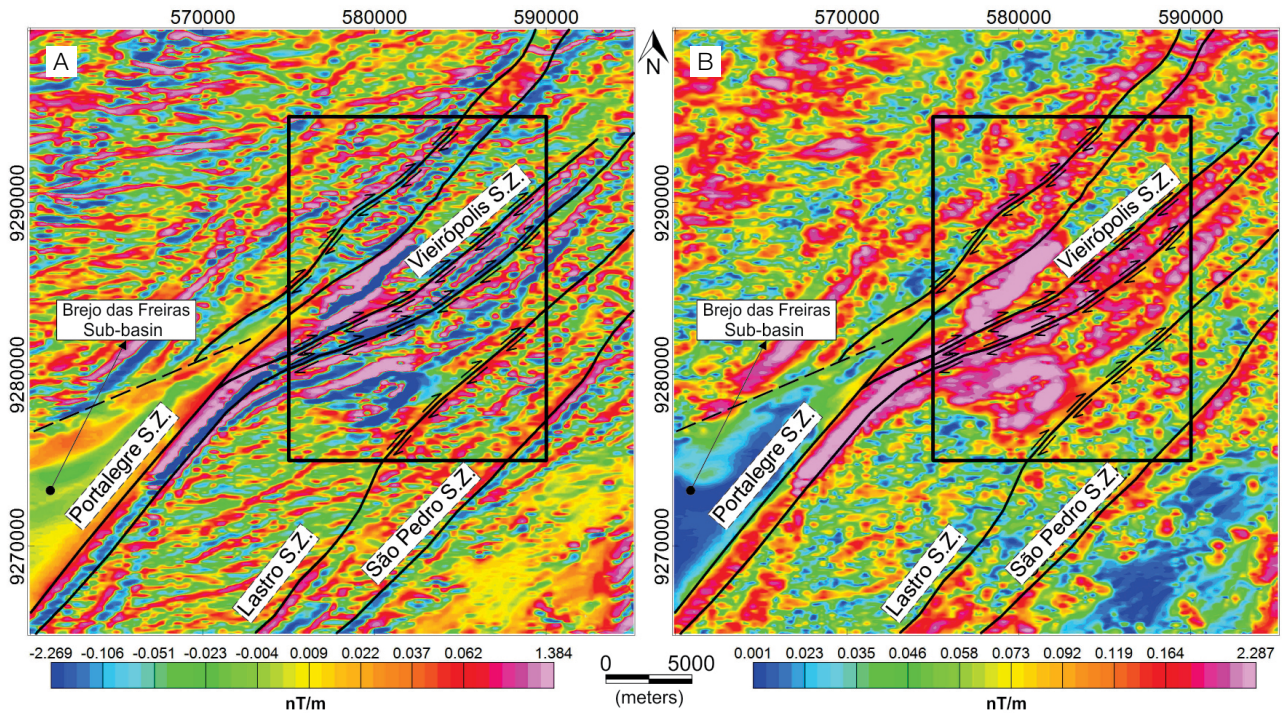


**Figure 10.** Magnetic lineaments, associated with shear zones of the study area, interpreted on the first vertical derivative of anomalous magnetic field (A), and by analytic signal amplitude (B). The structural correlation between the Portalegre and Vieirópolis shear zones can be observed, as well as the lateral continuity of the Lastro and São Pedro shear zones outside the study area. The dotted line delimits the upper edge of the Brejo das Freiras Sub-basin.

## ACKNOWLEDGEMENTS

The authors are grateful to the editors and reviewers, as well as to Daniel Machado, chief of the Publication Section of *Geologia USP – Série Científica*. We would like to express our gratitude to the Brazilian Geological Survey (CPRM-DISEGE) for the airborne geophysical data and CAPES for the scholarships granted to JFAN, GLS and IMBAS. We extend our thanks to *Mineração Limeira Comércio Exportação e Importação Ltda.* and *Granistone S/A* for the support given. Vanessa Ribeiro is also thanked for contributions in geophysical data acquisition.

## REFERENCES

- Acharyulu, A. A. P. S. R., Murty, B. S., Bhaumik, B. K. (2004). Enrichment characteristics of radioelements in various types of rock from Sambalpur district, Orissa, India. *Proceedings of the Indian Academy of Sciences, Earth and Planetary Sciences*, 113(3), 321-352. <https://doi.org/10.1007/BF02716729>
- Airo, M. L. (2013). Structural interpretation of airborne geophysical data: examples from Finland. Research Report. Finland: Geological Survey of Finland, 2/2013.
- Almeida, F. F. M., Hasui, Y., Brito Neves, B. B., Fuck, R. A. (1981). Brazilian structural provinces: an introduction. *Earth Sciences Reviews*, 17(1-2), 1-29. [https://doi.org/10.1016/0012-8252\(81\)90003-9](https://doi.org/10.1016/0012-8252(81)90003-9)
- Angelim, L. A. A. (Ed.). (2006). *Geologia e Recursos Minerais do Estado do Rio Grande do Norte*. Escala 1:500.000. Recife: CPRM/FAPER.
- Barreto, S. B., Muller, A., Araujo Neto, J. F., Bezerra, J. P. S., Souza, I. M. B. A., França, R. H. M., Santos, L. C. M. L. (2016). Vieirópolis Pegmatite Field, Northwest of Paraíba State, Brazil: New Occurrences of Amazonite Pegmatites. In: M. I. Jacobson (Ed.), *Second Eugene E. Foord Pegmatite Symposium: Abstracts, Short Papers, Posters and Program* (24-26). Denver: Friends of Mineralogy, Colorado Chapter.
- Batista, C. T., Verissimo, C. U. V., Amaral, W. S. (2014). Levantamento de feições estruturais lineares a partir de sensoriamento remoto – uma contribuição para o mapeamento geotécnico na Serra de Baturité, Ceará. *Geologia USP. Série Científica*, 14(2), 67-82. <http://dx.doi.org/10.5327/Z1519-874X201400020004>

- Brito Neves, B. B., Fuck, R. A., Pimentel, M. M. (2014). The Brasiliano collage in South America: a review. *Brazilian Journal of Geology*, 44(3), 493-518. <http://doi.org/10.5327/Z2317-4889201400030010>
- Brito Neves, B. B., Santos, E. J., Van Schmus, W. R. (2000). Tectonic History of the Borborema Province. In: U. G. Cordani, E. J. Milani, A. Thomaz Filho, D. A. Campos (Eds.), *Tectonic Evolution of South America* (151-182). Rio de Janeiro: SBG.
- Carrino, T. A., Souza Filho, C. R., S., Leite, E. P. (2007). Avaliação do uso de dados aerogeofísicos para mapeamento geológico e prospecção mineral em terrenos intemperizados: o exemplo de Serra Leste, Província Mineral de Carajás. *Revista Brasileira de Geofísica*, 25(3), 307-320. <http://doi.org/10.1590/S0102-261X2007000300007>
- Dantas, E. L., Silva, A. M., Almeida, T., Moraes, R. A. V. (2003). Old geophysical data applied to modern geological mapping problems: a case-study in the Seridó Belt, NE Brazil. *Revista Brasileira de Geociências*, 33, 65-72.
- Dickson, B. L., Scott, K. M. (1997). Interpretation of aerial gamma-ray surveys – adding the geochemical factors. *AGSO Journal of Australian Geology and Geophysics*, 17(2), 187-200.
- Drury, S. A. (2001). *Image Interpretation in Geology*. 3<sup>rd</sup> ed. Cheltenham: Nelson Thornes.
- Ferreira, C. A., Santos, E. J. (Orgs) (2000). *Programa Levantamentos Geológicos Básicos do Brasil. Jaguaribe SE. Folha SB.24-Z*. Escala 1:500.000. Recife: CPRM.
- Gomes, J. R. C., Vasconcelos, A. M., Torres, P. F. M. (2000). *Programa Levantamentos Geológicos Básicos do Brasil. Jaguaribe SW. Folha SB.24-Y*. Escala 1:500.000. Brasília: CPRM.
- Gundersen, L. C. S. (1991). Radon in sheared metamorphic and igneous rocks. In: L. C. S. Gundersen and R. B. Wanty (Eds.), *Field Studies of Radon in Rocks, Soils and Water. Geological Survey Bulletin*, 1971, 39-50. <https://doi.org/10.3133/b1971>
- Gunn, P. J. (1997). Quantitative methods for interpreting aeromagnetic data: a subjective review. *AGSO Journal of Australian Geology and Geophysics*, 17(2), 105-113.
- Hoff, R., Bastos Neto, A. C., Rolim, S. B. A. (2002). Contribuição do Estudo Aeromagnetométrico e de Imagens Orbitais (TM LANDSAT 5) ao Conhecimento do Arcabouço Geológico do Distrito Fluorítico de Santa Catarina (Brasil) e suas Implicações para a Prospecção de Fluorita. *Pesquisas em Geociências*, 29(2), 37-52.
- Jardim de Sá, E. F. (1994). *A Faixa Seridó (Província Borborema, NE do Brasil) e o seu significado geodinâmico na Cadeia Brasileira/Pan-Africana*. Tese (Doutorado). Brasília: Instituto de Geociências – UnB.
- Maas, M. V. R., Oliveira, C. G., Pires, A. C. B., Moraes, R. A. V. (2003). Aplicação da geofísica aérea na exploração mineral e mapeamento geológico do setor sudoeste do Cinturão Cuprífero Orós-Jaguaribe. *Revista Brasileira de Geociências*, 33(3), 279-288.
- Madrucci, V., Veneziani, P., Paradella, W. R. (2003). Caracterização geológica e estrutural através da interpretação do produto integrado TM-Landsat 5 e dados aerogamaespectrométricos, região de Alta Floresta – MT. *Revista Brasileira de Geofísica*, 21(3), 219-234.
- Medeiros, V. C. (Ed.) (2008). *Geologia e Recursos Minerais da Folha Sousa SB.24-Z-A*. Escala 1:250.000. Recife: CPRM.
- Medeiros, V. C., Amaral, C. A., Rocha, D. E. G. A. (2005). *Programa de Geologia do Brasil – PGB. Folha SB.24-Z-A Sousa*. Escala 1:250.000. Recife: CPRM.
- Medeiros, V. C., Medeiros, W. E., Jardim de Sá, E. F. (2011). Utilização de imagens aerogamaespectrométricas, Landsat 7 ETM+ e aeromagnéticas no estudo do arcabouço crustal da porção central do Domínio da Zona Transversal, Província Borborema, NE do Brasil. *Revista Brasileira de Geofísica*, 29(1), 83-97. <http://doi.org/10.1590/S0102-261X2011000100006>
- Milligan, P. R., Gunn, P. J. (1997). Enhancement and presentation of airborne geophysical data. *AGSO Journal of Australian Geology and Geophysics*, 17(2), 63-75.
- Moraes, J. F. S. (1999). *Gemas do Estado do Rio Grande do Norte*. Recife: CPRM.
- Nascimento, M. A. L., Galindo, A. C., Medeiros, V. C. (2015). Ediacaran to Cambrian magmatic suites in the Rio Grande do Norte domain, extreme Northeastern Borborema Province (NE of Brazil): Current knowledge. *Journal of South American Earth Sciences*, 58, 281-299. <http://doi.org/10.1016/j.jsames.2014.09.008>
- Neves, S. P. (2015). Constraints from zircon geochronology on the tectonic evolution of the Borborema Province (NE Brazil): Widespread intracontinental Neoproterozoic reworking of a Paleoproterozoic accretionary orogen. *Journal of South American Earth Sciences*, 58, 150-164. <https://doi.org/10.1016/j.jsames.2014.08.004>

- Neves, S. P., Bruguier, O., Silva, J. M. R., Bosch, D., Alcantara, V. C., Lima, C. M. (2009). The age distributions of detrital zircons in metasedimentary sequences in eastern Borborema Province (NE Brazil): Evidence for intracontinental sedimentation and orogenesis? *Precambrian Research*, 175, 187-205. <http://doi.org/10.1016/j.precamres.2009.09.009>
- Neves, S. P., Silva, J. M. R., Bruguier, O. (2017). Geometry, kinematics and geochronology of the Sertânia Complex (central Borborema Province, NE Brazil): assessing the role of accretionary versus intraplate processes during West Gondwana assembly. *Precambrian Research*, 298, 552-571. <https://dx.doi.org/10.1016/j.precamres.2017.07.006>
- Nóbrega, M. A. (2004). *Evolução estrutural e termocronológica meso-cenozóica da Zona de Cisalhamento Portalegre, Nordeste do Brasil*. Dissertação (Mestrado). Natal: Centro de Ciências Exatas e da Terra – UFRN.
- Oliveira, R. G. (2008). *Arcabouço geofísico, isostasia e causas do magmatismo cenozóico da Província Borborema e de sua Margem Continental (NE do Brasil)*. Tese (Doutorado). Natal: Centro de Ciências Exatas e da Terra – UFRN.
- Padilha, A. L., Vitorello, Í., Pádua, M. B., Fuck, R. A. (2016). Deep magnetotelluric signatures of the early Neoproterozoic Cariris Velhos tectonic event within the Transversal sub-province of the Borborema Province, NE Brazil. *Precambrian Research*, 275, 70-83. <http://ib.adnx.com/seg?add=1&redir=http%3A%2F%2Fdx.doi.org%2F10.1016%2Fj.precamres.2015.12.012>
- Paradella, W. R., Bignelli, P. A., Veneziani, P., Pietsch, R. W., Toutin, T. (1997). Airborne and spaceborne Synthetic Aperture Radar (SAR) integration with Landsat TM and gamma ray spectrometry for geological mapping in a tropical rainforest environment, the Carajás Mineral Province, Brazil. *International Journal of Remote Sensing*, 18(7), 1483-1501. <https://doi.org/10.1080/014311697218232>
- Ribeiro, V. B., Mantovani, M. S. M., Louro, V. H. A. (2013). Aerogamaespectrometria e suas aplicações no mapeamento geológico. *Terrae Didatica*, 10, 29-51. <https://doi.org/10.20396/td.v10i1.8637386>
- Roest, W. R., Verhoef, J., Pilkington, M. (1992). Magnetic interpretation using the 3-D analytic signal. *Geophysics*, 57, 116-125. <https://doi.org/10.1190/1.1443174>
- Santos, E. J. (1996). Ensaio preliminar sobre terrenos e tectônica acrescionária na Província Borborema. *XXXIX Congresso Brasileiro de Geologia*, 6, 47-50. Salvador: SBG.
- Santos, E. J., Souza Neto, J. A., Silva, M. R. R., Beurlen, H., Cavalcanti, J. A. D., Silva, M. G., Dias, V. M., Costa, A. F., Santos, L. C. M. L., Santos, R. B. (2014). Metalogênese das porções norte e central da Província Borborema. In: M. G. Silva, M. B. Rocha Neto, H. Jost, R. M. Kuyumijan (Eds.), *Metalogênese das províncias tectônicas brasileiras*, 343-388. Belo Horizonte: CPRM.
- Santos, L. C. M. L., Dantas, E. L., Vidotti, R. M., Cawood, P. A., Santos, E. J., Fuck, R. A., Lima, H. M. (2017). Two-stage terrane assembly in Western Gondwana: Insights from structural geology and geophysical data of central Borborema Province, NE Brazil. *Journal of Structural Geology*, 103, 167-184. <https://doi.org/10.1016/j.jsg.2017.09.012>
- Serviço Geológico do Brasil (CPRM). (2009). *Projeto Aerogeofísico Paraíba - Rio Grande do Norte; Pernambuco - Paraíba*. Rio de Janeiro: Lasa Engenharia e Prospecções, Prospectores Aerolevantamentos e Sistemas.
- Souza, L. C., Sá, J. M., Legrand, J. M., Maia, H. N. (2011). *Programa de Geologia do Brasil – Carta Geológica Folha SB.24-Z-A-II Pau dos Ferros*. Escala 1:100.000. Brasília: CPRM.
- Stewart, J. R., Betts, P. G., Collins, A. S., Schaefer, B. F. (2009). Multi-scale analysis of Proterozoic shear zones: An integrated structural and geophysical study. *Journal of Structural Geology*, 31, 1238-1254. <https://doi.org/10.1016/j.jsg.2009.07.002>
- Van Schmus, W. R., Kozuch, M., Brito Neves, B. B. (2011). Precambrian history of the Zona Transversal of the Borborema Province, NE Brazil: Insights from Sm-Nd and U-Pb geochronology. *Journal of South American Earth Sciences*, 31, 227-252. <http://dx.doi.org/10.1016/j.jsames.2011.02.010>
- Van Schmus, W. R., Oliveira, E. P., Silva Filho, A. F., Toteu, S. F., Penaye, J., Guimarães, I. P. (2008). Proterozoic links between the Borborema Province, NE Brazil and the Central African Fold Belt. *Geological Society – Special Publications*, 294, 69-99. <https://doi.org/10.1144/SP294.5>
- Zacchi, E. N. P., Silva, A. M., Rolim, V. K. (2010). Análise integrada de dados multifonte e sua aplicação no mapeamento geológico das formações ferríferas da Serra de Itapanhoacanga, Alvorada de Minas, MG. *Revista Brasileira de Geofísica*, 28(4), 643-656. <http://dx.doi.org/10.1590/S0102-261X2010000400009>